Cascade enzymatic cleavage of the β-O-4 linkage in a lignin model compound†

Elena Rosini,*[ab] Chiara Allegretti,[c] Roberta Melis,[a] Lorenzo Cerioli,[c] Gianluca Conti,[a] Loredano Pollegioni[ab] and Paola D'Arrigo*[bcd]

The β-O-4 aryl ether linkages represent about 50% of all ethers in various lignins. At least three enzymatic steps are required to break them down: a NAD+-dependent C-α dehydrogenase (such as LigD and L), a glutathione lyase that releases guaiacol (i.e.,aβ-etherase such as LigE and F), and a glutathione-dependent lyase (i.e.,LigG).InthisworktheLigD,L,E,F,andGfromSphingobium sp. SYK-6 were overexpressed in E. coli and purified with high yields. After characterizing the stability and kinetic properties of LigD and L on the lignin model compound GGE (1-(4-hydroxy-3-methoxyphenyl)-2-(2-methoxyphenoxy)propane-1,3-diol) and the thermostability of all five recombinant Lig enzymes, the experimental conditions for GGE bioconversion could be optimized (i.e.,pH9.0,25°C, ≈0.1 mg mL−1 of each enzyme, and 0.5 mM racemic substrate). Under optimal conditions, and by recycling NADH using the L-lactate dehydrogenase–pyruvate system, GGE was fully converted into the final products 3-hydroxy-1-(4-hydroxy-3-methoxyphenyl)propan-1-one and guaiacol in <2 hours. Differently from what was previously reported, this result and chiral HPLC analyses demonstrated that LigG catalyzes the glutathione-dependent thioether cleavage of both β(R)- and β(S)-isomer intermediates produced by LigE and LigF β-etherases: this allowed, for the first time, reaching 100% conversion of GGE. Altogether, the recombinant five-enzyme Lig system represents a component well suited for a multienzymatic process, comprising well-known ligninolytic activities (such as peroxidases and laccases), devoted to transforming selected lignins into aromatic compounds as an alternative to the oil source.

1. Introduction

Lignocellulose refers to plant dry matter (biomass or the so-called lignocellulosic biomass). It is composed of carbohydrate polymers (cellulose, hemicellulose) and an aromatic polymer (lignin) and represents the most promising feedstock. Although burning lignin still represents a valuable contribution for saving fossil sources, lignin also offers perspectives in terms of higher value-added applications. In fact, after the hydrolysis of lignocellulose polysaccharides, lignin remains as a solid residue, representing one of the major renewable sources for biofuel and fine chemical (mainly aromatics) production. The main limitation to practical applications for lignin so far is presumably due to the difficult and challenging processing for depolymerization and valorization. In this respect, lignin can be depolymerized by chemical means (*e.g.*, thermochemical methods such as pyrolysis, chemical oxidation, hydrogenolysis, gasification, and hydrolysis under supercritical conditions):[1] these processes are energy-consuming, environmentally unfriendly, and generate a complex mixture of degraded and partially repolymerized products. As a suitable alternative, lignin valorization can be obtained by cleaving selected bonds under mild conditions using enzymatic approaches.[2,3] Known ligninolytic enzymes include peroxidases (such as heme-dependent lignin peroxidases, manganese peroxidases, and versatile peroxidases) and laccases.[4,5] Taking into account that lignin is constituted by phenylpropane units linked by ether and carbon–carbon bonds, in addition to these oxidative enzymes, nonradical ligninolytic enzymes represent a specific and effective alternative for lignin cleavage and valorization. Since the β-aryl ether bonds account for up to 50% of the ethers in lignin, cleavage of such linkages by using β-etherases would produce valuable,

[a] *Dipartimento di Biotecnologie e Scienze della Vita, Università degli Studi dell'Insubria, Via J.H. Dunant 3, 21100 Varese, Italy.*
E-mail: elena.rosini@uninsubria.it; Fax: +39 0332421500
[b] *The Protein Factory, Politecnico di Milano and Università degli Studi dell'Insubria, Via Mancinelli 7, 20131 Milano, Italy*
[c] *Dipartimento di Chimica, Materiali e Ingegneria Chimica "Giulio Natta", Politecnico di Milano, Piazza Leonardo da Vinci 32, 20133 Milano, Italy.*
E-mail: paola.d'arrigo@polimi.it; Fax: +39 0223993180
[d] *Istituto di Chimica del Riconoscimento Molecolare, CNR, Via Mario Bianco 9, 20131 Milano, Italy*

† Electronic supplementary information (ESI) available: Synthesis of compounds **1**–**4** and **9**, SDS-PAGE analysis of the purified recombinant Lig enzymes, mass spectra of compound **9**, and HPLC calibration curves.

Received: 21st September 2015,
Accepted: 2nd November 2015

industrially useful, low-molecular-mass aromatic compounds as important building blocks for preparative organic chemistry. Up to now, β-etherases have been reported in an ascomycete of the genus *Chaetomium*,[6] in *Sorangium cellulosum* So Ce56,[7] in the soil α-proteobacterium *Sphingobium paucimobilis* SYK-6,[8] in *Novosphingobium* sp. PP1Y, and in *Novosphingobium aromaticivorans* DSM1244.[7] The β-aryl ether degradation pathway of *S. paucimobilis* SYK-6 requires the presence of nicotinamide adenine dinucleotide (NAD^+)-dependent, stereospecific alcohol dehydrogenases (LigD, LigL, LigN, and LigO), which catalyze the initial oxidation of the α-hydroxyl group in the typical model substrate 1-(4-hydroxy-3-methoxyphenyl)-2-(2-methoxyphenoxy)propane-1,3-diol (GGE, **1**–**4**) to the corresponding ketone 3-hydroxy-1-(4-hydroxy-3-methoxyphenyl)-2-(2-methoxyphenoxy)propan-1-one (**5**–**6**) (see Scheme 1). LigD and LigO convert the (1*R*,2*R*) and (1*R*,2*S*) isomers of GGE (**1** and **2**) into the (*R*) and the (*S*) isomers (compounds **5** and **6** in Scheme 1), whereas LigL and LigN enzymes catalyze the conversion of the (1*S*,2*R*) and (1*S*,2*S*) isomers of GGE (**3** and **4**) to the (*R*) and (*S*) isomers.[9] Subsequently, LigE, LigF, and LigP catalyze the nucleophilic attack by glutathione (GSH) on the β-carbon atom of substrates containing β-aryl ether linkages to produce a GSH-conjugated aromatic compound 3-hydroxy-1-(4-hydroxy-3-methoxyphenyl)-2-(*S*-glutathionyl)propan-1-one (**7** and **8**) and 2-methoxyphenol (guaiacol). These LigE, LigF, and LigP enzymes belong to the glutathione transferase superfamily (GSTs; EC 2.5.1.18), whose members are involved in a broad range of detoxifying

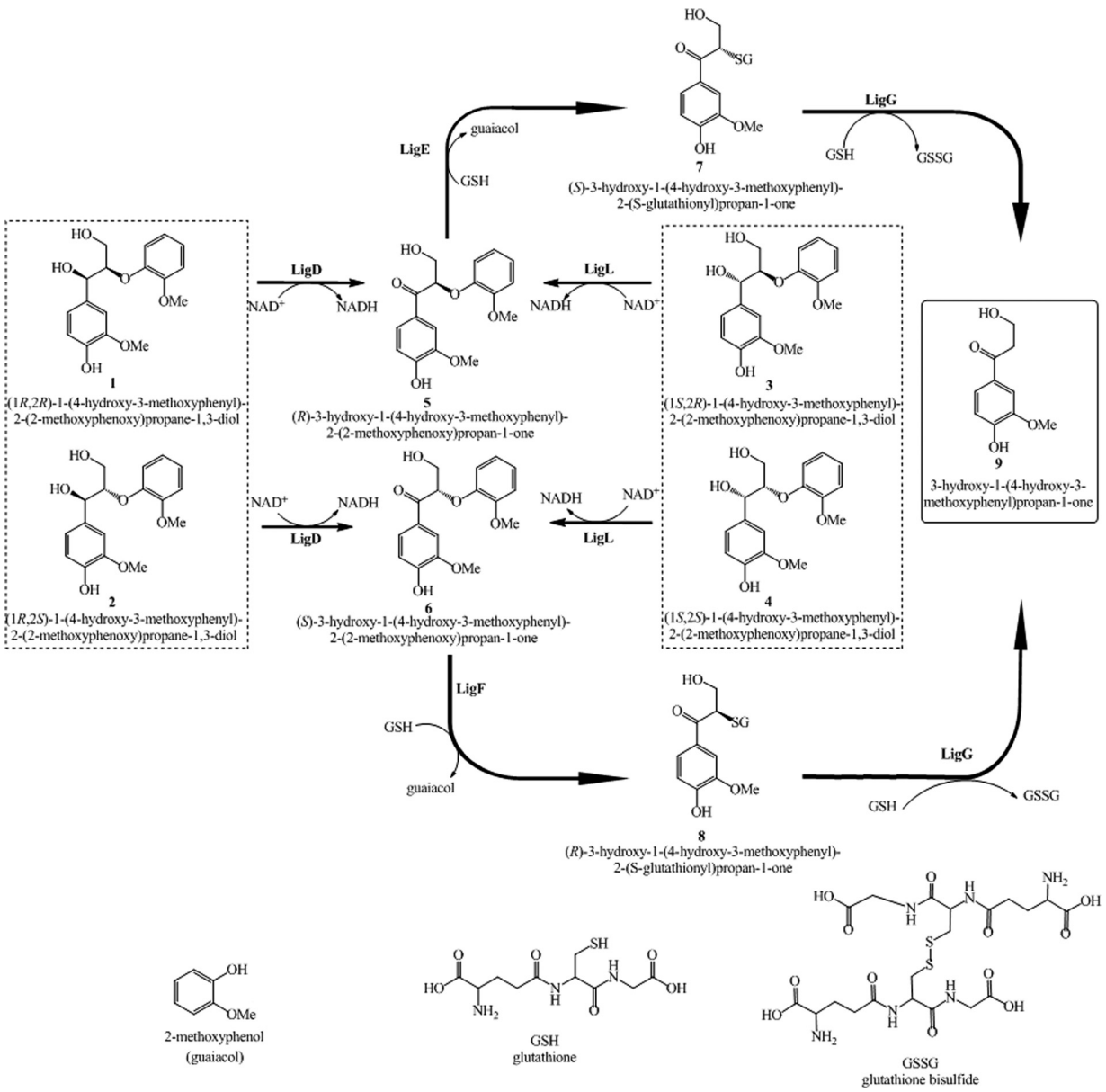

Scheme 1 Degradation of the stereoisomers of 1-(4-hydroxy-3-methoxyphenyl)-2-(2-methoxyphenoxy)propane-1,3-diol (GGE, **1**–**4**) catalyzed by the Lig enzymatic system.

processes. These β-etherases are also stereoselective and selectively attack the two enantiomers of a racemic mixture of **5** and **6**, producing the stereochemical inversion of chiral β-carbon: LigF produces the (*R*)-glutathionyl derivative **8** from (*S*)-ketone **6**, while LigE and LigP are selective for (*R*)-ketone **5** to provide the (*S*)-glutathionyl compound **7**.[10] The last step of the process is carried out by LigG (EC 2.5.1.18), a glutathione-lyase belonging to the omega class of glutathione transferases[11] that, in the presence of GSH, catalyzes a stereoselective thioether cleavage to produce oxidized glutathione (GSSG) and 3-hydroxy-1-(4-hydroxy-3-methoxyphenyl)propan-1-one (**9**).

Among the β-etherases, only LigF has been biochemically characterized so far.[12,13] The substrate preference of LigD from *Sphingobium* sp. SYK-6 was recently investigated,[14] demonstrating that it oxidizes genuine dilignols and GGE derivatives into the corresponding α-keto products.

Notably, LigD tolerates variations in the side chains and accepts bulky, aromatic ring phenolic substitutions in the β-O-4 substrates and oxidizes synthetic β-O-4 lignin oligomers, thus performing both end- and internal-unit oxidations. Indeed, purified LigD, F, and G were used to assess the release of monomers and the polymer distribution of two technical lignins: GPC analysis showed a minimal increase in low-molecular-weight compounds (at 120–200 MW) and an increase in the high-molecular-weight fraction in both lignin samples used; a slight increase in the fraction of compounds at 300 MW was only observed in softwood alkali-lignin.[12] In this work we report on the optimization of recombinant expression in *E. coli* of five enzymes with different stereoselectivity, namely, LigD, L, E, F, and G from *Sphingobium* sp. SYK-6 and their biochemical characterization. The information obtained was then used to optimize the full bioconversion process of a racemic mixture of GGE.

2. Results and discussion

2.1 Expression and purification of Lig enzymes

The synthetic cDNAs encoding for LigD, L, E, F, and G enzymes, whose codon usage was optimized for protein expression in *E. coli*, were cloned in pET24b(+) plasmid to yield the pET24-Lig expression plasmids. Recombinant enzymes containing a His-tag at the C-terminus were produced as detailed in the Experimental section and were purified in a single step by HiTrap chelating chromatography: recombinant LigD, L, E, F, and G enzymes were isolated as a single band at ≈31–33 kDa, with >90% purity as judged by SDS-PAGE analysis (Fig. S1 of the ESI†): ≈60, 20, 80, 60, and 55 mg of purified enzyme per L of fermentation broth were obtained, respectively.

The specific activities of purified LigD and LigL enzymes with a racemic mixture of GGE as substrate (at a fixed 0.5 mM final concentration, pH 9.0, 25 °C) were 32.1 U mg^{-1} and 38.5 U mg^{-1}, respectively. A value of 12 U mg^{-1} protein was reported for LigD at pH 9.0 and 45 °C by Reiter *et al.*[12]

2.2 Biochemical properties of LigD and LigL enzymes

The apparent kinetic parameters of recombinant NAD^+-dependent LigD and LigL enzymes were determined on the GGE racemic mixture as substrate, at 25 °C in 20 mM sodium acetate buffer, pH 9.0, in the presence of 0.5 mM NAD^+ (Table 1).

In both cases, the dependence of the reaction rate on the substrate concentration followed Michaelis–Menten kinetics: a classical 'inhibition by substrate' (*i.e.*, the activity decreases at high substrate concentrations) was apparent at substrate concentrations >0.5 mM (Fig. 1).

Notably, such an effect was not apparent at 45 °C (not shown), as also previously reported up to 2.5 mM GGE by Reiter *et al.*[12] The binding of the oxidized form of the cofactor was assessed spectrofluorimetrically by following the perturbation of the protein emission spectrum of LigD and LigL upon formation of the enzyme–ligand complex. The K_d values, summarized in Table 1, indicate a significantly tighter binding of NAD^+ for LigL enzyme (up to 4-fold) than for LigD enzyme.

The temperature dependence of the enzymatic activity of LigD and LigL on GGE as substrate was assayed in the 15–60 °C range. As shown in Fig. 2, both enzymes show the highest activity at 37 °C (up to 2.5-fold in comparison to the value obtained at 25 °C for LigL) and at pH 9.0.

The two dehydrogenases are active at low temperatures; the enzymatic activity is lost at ≥60 °C and at pH ≤ 6.0 (Fig. 2).

Notably, under our experimental conditions the temperature optimum of LigD differs significantly from that reported by Reiter *et al.*,[12] *i.e.*, 60 °C at pH 9.0, while the pH activity is similar.

Concerning stability, LigD is fully stable after incubation for 24 h at 25 °C and shows a ≈80% residual activity when the temperature was raised to 37 °C and 45 °C. Moreover, this enzyme possesses good stability at all pH values tested (in the 4–9 range). In contrast, LigL is not stable at 37 and 45 °C: the enzymatic activity is completely abolished after 10 min of incubation at these temperatures. LigL shows a ≈35% residual activity after incubation for 18 h at 25 °C; interestingly, a significantly higher value (≈55%) is assayed when the incubation mixture contained 0.5 mM NAD^+.

2.3 Structural characterization of Lig enzymes

The five Lig enzymes obtained as recombinant proteins show only minor differences in the visible absorbance spectra (not shown). In contrast, spectral properties depending on the protein folding (protein fluorescence and UV CD spectra) profoundly distinguish the different Lig enzymes. As shown in Fig. 3A, tryptophan emission at 340 nm (following excitation at 280 nm) is ≈3-fold lower for the two dehydrogenases (LigD and LigL) than for the other Lig enzymes. Based on the number of Trp residues, LigE may possess the highest fluorescence, followed by LigF and LigG (11, 8, and 6 Trp residues each): notably, quenching interactions between tryptophan side chains and nearby side chains are less relevant for the

Table 1 Apparent kinetic parameters on GGE racemic mixture as substrate and dissociation constant for NAD^+ of LigD and LigL enzymes. The activity was assayed at a fixed 0.5 mM NAD^+ concentration, pH 9.0 and 25 °C

	$V_{max,app}$ [U mg^{-1}]	K_m [mM]	V_{max}/K_m [U mg^{-1} mM^{-1}]	K_i [mM]	K_d NAD^+ [mM]
LigD	35 ± 1.2	0.12 ± 0.05	292	2.5 ± 0.7	0.29 ± 0.02
LigL	46 ± 1.5	0.04 ± 0.01	1150	4.0 ± 0.5	0.07 ± 0.01

latter enzyme since its fluorescence yield is quite similar to that of LigE even if it contains half of the Trp residues. Similarly, the protein fluorescence determined for the LigD is higher than that for LigL although it only contains two Trp residues (*vs.* three for the latter, see Fig. 3A). Far- and near-UV CD spectra reveal a major difference in the features related to the secondary and tertiary structures of different Lig enzymes (see Fig. 3B and C). The *in vitro* interaction between Lig enzymes was investigated by size exclusion chromatography and CD spectral analysis on different enzyme mixtures (*i.e.*, LigD, F, G or LigL, E, G, at 0.1 mg mL^{-1} of each protein). Gel permeation chromatography does not show any evidence of protein interaction since no peaks corresponding to complexes at higher molecular mass were observed (data not shown). Similarly, no changes in the near-UV CD spectrum of each enzyme were observed when the β-etherase and then the glutathione lyase were added to the dehydrogenase (data not shown). Taken together, these results exclude the formation of a stable complex between the investigated Lig enzymes.

Studies on the temperature sensitivity of tryptophan fluorescence (taken as a reporter of tertiary structure modifications) gave T_m values close to those obtained by following far-UV CD signals (a probe of secondary structure modification, Table 2). Midpoint transition temperatures as detected by the various experimental approaches were always ≈10–15 °C lower for LigL than for the other Lig enzymes (Table 2). This is in good agreement with the lower stability observed for this dehydrogenase at temperatures ≥37 °C (see above).

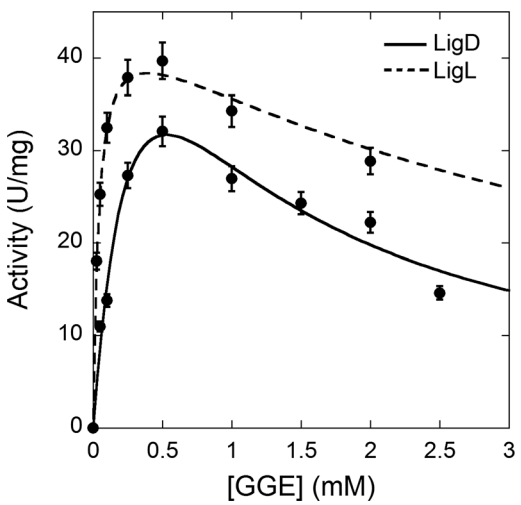

Fig. 1 Dependence of LigD and LigL activity on the concentration of GGE (racemic mixture). The data points were obtained as described in the text (average of at least 3 single measurements) and determined using 3 μg of enzyme per assay. The curves are from fits based on the classical Michaelis–Menten equation modified to account for a substrate inhibition effect.

2.4 Bioconversion of GGE

2.4.1 Set-up of the enzymatic process. The Lig enzymatic system from strain *S. paucimobilis* SYK-6 acts on the model substrate 1-(4-hydroxy-3-methoxyphenyl)-2-(2-methoxyphenoxy)propane-1,3-diol (GGE, which is composed of 4 stereoisomers, **1**–**4**) in a stereoselective manner (see Scheme 1). Substrate degradation involves different steps which also require NAD^+ and glutathione (GSH) to produce 3-hydroxy-1-(4-hydroxy-3-methoxyphenyl)propan-1-one (**9**) as the final product. Formation of the GGE degradation products by the Lig system (0.1 mg mL^{-1} of each enzyme, final concentration, if not indicated otherwise) was determined by HPLC analysis and the intermediates and the final product were also characterized by ESI-MS and ^1H NMR.

When 0.5 mM GGE was incubated with pure recombinant LigD in 20 mM ammonium acetate buffer, pH 9.0, in the presence of NAD^+, ≈57% of the initial GGE is unreacted after 30 min, in agreement with the known ability of this dehydrogenase to oxidize the stereoisomers with the (1*R*) configuration (compounds **1** and **2** in Scheme 1) into the respective ketones (*R*)-3-hydroxy-1-(4-hydroxy-3-methoxyphenyl)-2-(2-methoxyphenoxy)propan-1-one (**5**) and (*S*)-3-hydroxy-1-(4-hydroxy-3-methoxyphenyl)-2-(2-methoxyphenoxy)propan-1-one (**6**).[9,12] The optimal pH and temperature for the LigD-catalyzed degradation of GGE

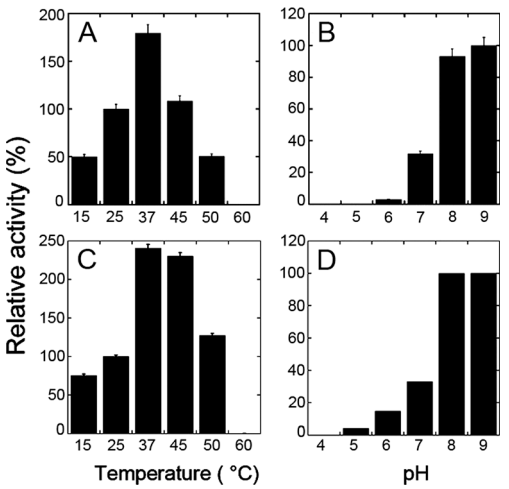

Fig. 2 Effect of temperature and pH on the enzymatic activity of LigD (A, B) and LigL (C, D) enzymes on GGE as substrate. The activity values at 25 °C and pH 9.0 were taken as 100%.

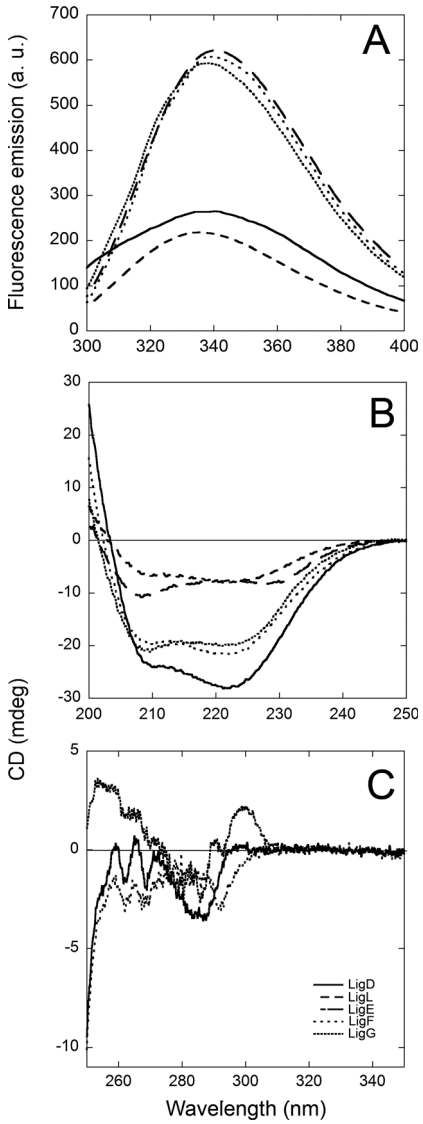

Fig. 3 Spectral analysis of secondary and tertiary structures of Lig enzymes. A) Comparison of protein fluorescence of different Lig enzymes. Fluorescence spectra were recorded from 300 to 400 nm with excitation at 280 nm. Samples of Lig enzymes (0.1 mg mL^{-1}) were equilibrated at 15 °C in 50 mM Tris–HCl, pH 7.5, 10% glycerol. B) Far-UV CD spectrum of different Lig enzymes (0.1 mg protein per mL). Estimating the protein secondary structure by means of K2D3 software indicates that the α-helix content for LigL, E, F, and G enzymes is 14%, 27%, 67%, and 64% and the β-strand content is 2%, 35%, 21%, and 2%, respectively. C) Near-UV CD spectrum of different Lig enzymes (0.4 mg protein per mL). In (B) and (C), proteins were in 50 mM Tris–HCl, pH 7.2; measurements were performed at 15 °C.

were estimated to be 9.0 and 45 °C (*e.g.*, at pH 7.5 in 20 mM potassium phosphate buffer only 26% of GGE was converted after 22 h). Moreover, if GGE was incubated under the same experimental conditions without LigD, no reaction occurred after 24 h or in the presence of 0.5 mM NAD^+ and 0.5 mM GSH.

Conversely, if 0.5 mM GGE was incubated with LigL in the presence of ≈0.2 mM NAD^+, 40% of ketones were produced in 30 min at pH 9.0 and 25 °C, again confirming the ability

Table 2 Comparison of T_m values as determined by following tryptophan fluorescence and far-UV CD spectra for different Lig enzymes

Method	Enzyme	T_m [°C]
Trp fluorescence	LigD	59.1 ± 0.2
	LigL	44.2 ± 0.1
	LigE	55.3 ± 0.3
	LigF	55.0 ± 0.3
	LigG	47.9 ± 0.1
Far-UV CD (220 nm)	LigD	53.7 ± 0.1
	LigL	41.2 ± 0.2
	LigE	53.6 ± 0.1
	LigF	59.0 ± 0.1
	LigG	50.8 ± 0.1

of the dehydrogenase to oxidize isomers **3** and **4** only (*i.e.* the ones having carbon 1 in the (*S*) configuration).[9] In this case, a lower reaction temperature was required than with LigD, since LigL was not stable at 45 °C for the time required to complete the bioconversion. To test the stereoselectivity of the β-etherase activity of LigE and LigF, we incubated the synthesized racemic mixture of ketones (**5** + **6**) in the presence of each single enzyme with glutathione and LigG. The chiral HPLC analysis of both reaction mixtures showed clearly that only one enantiomer disappeared in each case (see Fig. 4A and B): the peak with a $t_{(R)}$ of 18.2 min disappeared in the presence of LigF, thus representing (*S*)-3-hydroxy-1-(4-hydroxy-3-methoxyphenyl)-2-(2-methoxyphenoxy)propan-1-one (**6**). In contrast, the peak with a $t_{(R)}$ of 22 min disappeared in the presence of LigE, showing that it is related to (*R*)-3-hydroxy-1-(4-hydroxy-3-methoxyphenyl)-2-(2-methoxyphenoxy)propan-1-one (**5**) (Fig. 4A and C). In both cases the final product **9** appeared at a $t_{(R)}$ of about 14.3–14.5 min, the same elution volume of the standard (see Fig. 4D). Its identity was also confirmed by MS analysis (see comparison of the spectra for compound **9** obtained by chemical synthesis and the one from LigG bioconversion in Fig. S2†).

Indeed, a 60 min reaction of LigD and LigF on racemic GGE in the presence of 0.5 mM NAD^+ and 0.5 mM GSH (in 20 mM ammonium acetate buffer, pH 9.0, at 45 °C) produced the (*R*)-3-hydroxy-1-(4-hydroxy-3-methoxyphenyl)-2-(*S*-glutathionyl) propan-1-one (**8**) without formation of the final product (**9**), which instead appeared when LigG was also added to the reaction mixture (Fig. 5A–C). Notably, the LigF catalysis caused inversion of the configuration at carbon β. On the other hand, after incubation of GGE with LigL and LigE (in 20 mM ammonium acetate buffer, pH 9.0, at 25 °C) the enantiomer of compound **8**, namely (*S*)-3-hydroxy-1-(4-hydroxy-3-methoxyphenyl)-2-(*S*-glutathionyl)propan-1-one (**7**), was formed in 30 min. This enantiomer was then cleaved in the presence of LigG and GSH, producing the final product **9** (Fig. 5A, D and E). When the reaction mixtures containing the glutathione conjugates **7** and **8** (produced by the β-etherases LigE and LigF, respectively) were treated with an excess of glutathione (1 mM) in order to force the equilibrium *versus* the formation of the final product, no formation of **9** was apparent: the thioether cleavages only occurred in

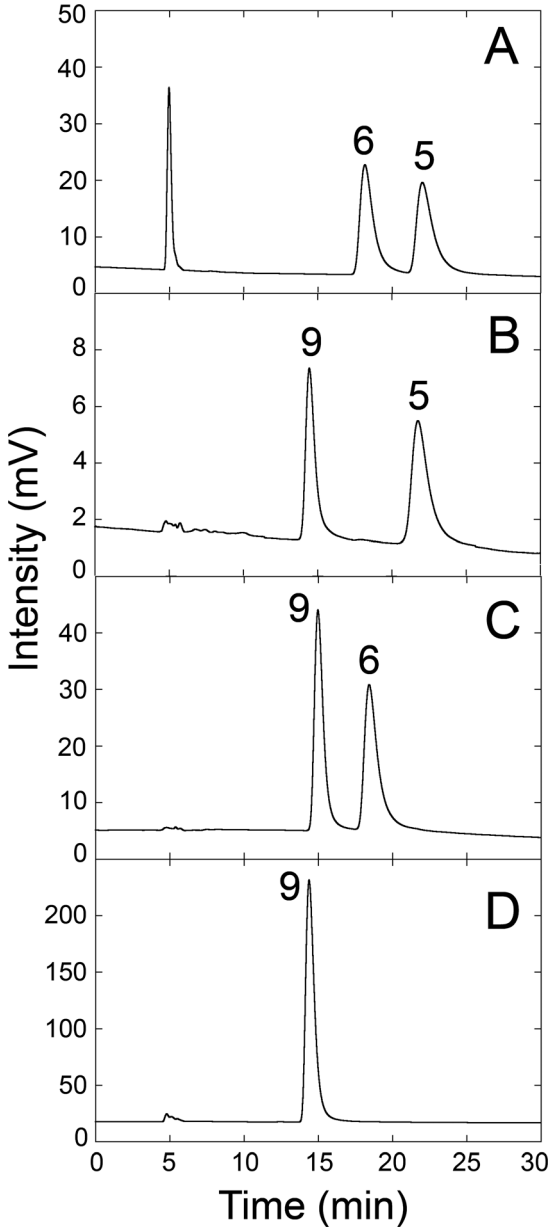

Fig. 4 Chiral HPLC analysis of LigE or LigF catalyzed enantioselective reaction of racemic 3-hydroxy-1-(4-hydroxy-3-methoxyphenyl)-2-(2-methoxyphenoxy)propan-1-one (**5** + **6**). A) The initial mixture of racemic (**5** + **6**) prior to the addition of enzymes; B) after 24 h of incubation with LigF, LigG and 0.5 mM GSH; C) after 24 h of incubation with LigE, LigG and 0.5 mM GSH; D) pure, synthesized product **9**.

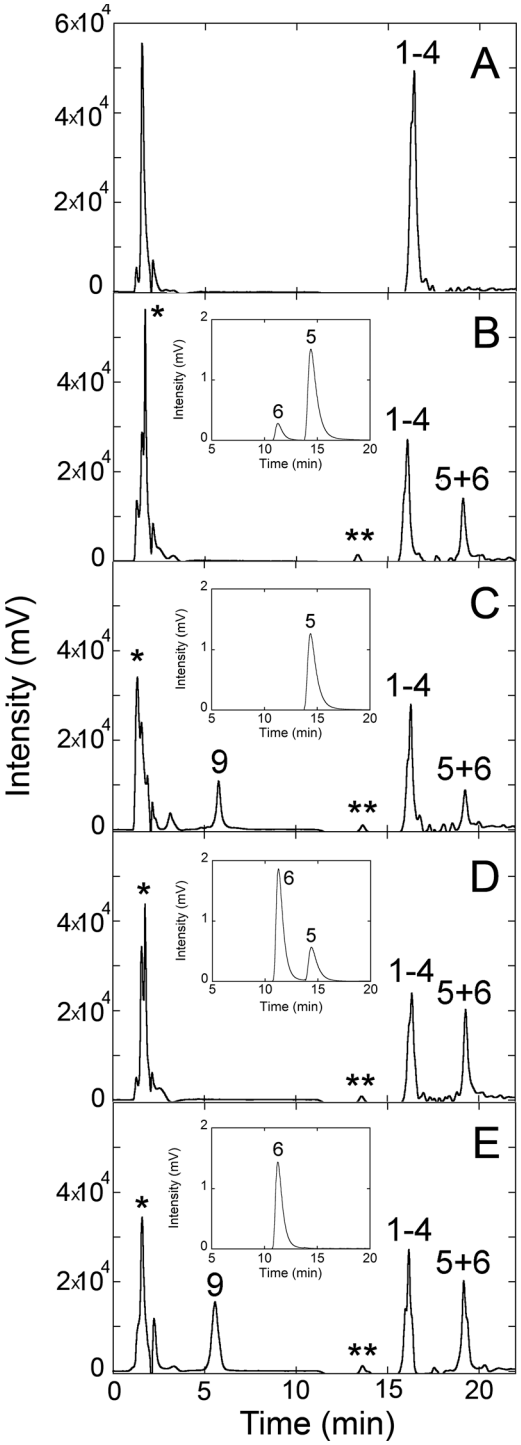

Fig. 5 HPLC chromatograms of GGE prior to the addition of enzymes (A), following bioconversion catalyzed by LigD and LigF (B), and the subsequent addition of LigG (C). Bioconversion of GGE catalyzed by LigL and LigE (D) and subsequent addition of LigG (E). Note: the peak * at 1.7 min contains the NAD^+/NADH cofactor and the intermediates **7** and **8**; the peak ** at 14.5 min contains guaiacol. The insets represent the chiral analysis of the peak marked as 5 + 6.

the presence of LigG. Surprisingly, and differently from that previously reported,[10] LigG cleaves both thioethers **7** and **8** in the presence of GSH without apparent stereoselectivity.

2.4.2 Multienzymatic cascade bioconversion. 0.5 mM GGE was incubated with the complete enzymatic system LigD, L, F, E, and G, in the presence of 1 mM NAD^+ and 2 mM GSH, in 20 mM ammonium acetate buffer at pH 9.0 and 25 °C. After 2 h GGE was fully transformed in the final product **9** with a ≈100% yield (Fig. 6A and B). However, when GGE was enzymatically converted in the absence of LigG, the reaction mixture contained ≈60% of unreacted GGE after 18 h, without formation of the final product **9**: after subsequently adding LigG all intermediates were completely converted to the final product (Fig. 6C and D). These results demonstrated

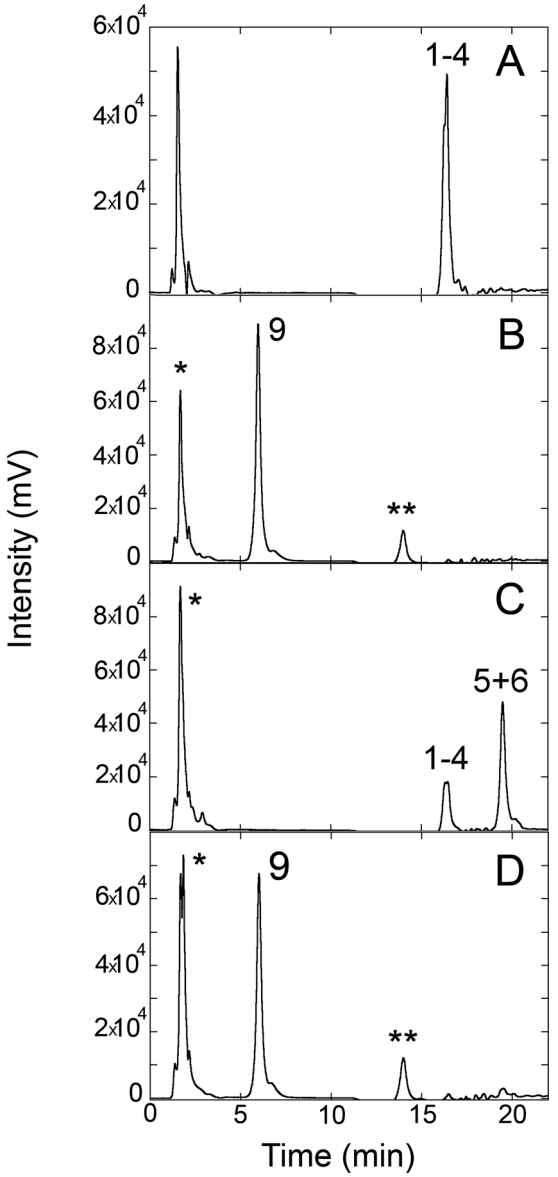

Fig. 6 HPLC chromatograms of GGE prior to the addition of enzymes (A), following bioconversion catalyzed by LigD, L, E, F, G (2 h at 25 °C and pH 9.0) (B), or following bioconversion catalyzed by LigD, L, E, F (12 h at 25 °C and pH 9.0) (C) and 240 min after the addition of LigG to this reaction mixture (D). Note: the peak * at 1.7 min contains the NAD^+/NADH cofactor and the intermediates **7** and **8**; the peak ** at 14.5 min contains guaiacol.

that the full degradation of GGE is feasible using the 5 enzymes at pH 9.0 and 25 °C, a condition compatible with the stability of all enzymes and that avoids reaction equilibria.

In view of a practical application, the Lig bioconversion of GGE has been optimized by recycling NADH in the presence of L-lactate dehydrogenase (LDH) and pyruvate, at pH 9.0 and 25 °C (see Fig. 7A). A faster time course of GGE conversion was obtained when NAD^+ was recycled, *i.e.*, at lower NAD^+ concentration (0.5 mM) with a higher accumulation of intermediates (**5** + **6**) (Fig. 7B, right). In contrast, the rate of production of compound **9** was similar for both procedures. Under these conditions, the quantity of NAD^+ can be significantly decreased, allowing a consistent reduction in the cost of the overall bioconversion system.

3. Experimental section

3.1 Design and cloning of cDNAs encoding for Lig enzymes

The synthetic cDNAs encoding for LigD, LigL, LigE, LigF, and LigG enzymes from *Sphingobium* sp. SYK-6 (ref. 9 and 12) were designed by *in silico* back translation of the amino acid sequences reported in the GenBank database (accession no. BAA01953.1, YP004836498.1, YP004833998.1, BAA02031.1 and BAA77216.1, respectively).

In order to facilitate subcloning into the pET24b(+) plasmid, sequences corresponding to *Nde*I (CATATG) and *Xho*I (CTCGAG) restriction sites were added at the 5′- and 3′-ends of the cDNAs, respectively. The codon usage of the synthetic cDNAs was optimized for expression in *E. coli*; genes were produced by GeneArt (Life Technologies, Monza, Italy) (accession no. KR868729, KR868732, KR868733, KR868730 and KR868731, respectively). *lig* cDNAs were inserted in the pET24b(+) vector using the *Nde*I and *Xho*I sites; six codons (encoding for six additional histidines) were added to the 3′-end of the *lig* genes during the subcloning process.

3.2 Expression and purification of Lig enzymes

The pET24-Lig plasmids were transferred to the host BL21(DE3) *E. coli* strain. Cells were grown at 37 °C in LB medium. Protein expression was induced at an OD_{600nm} ≈1.2 by adding 1 mM IPTG; the cells were further grown at 25 °C for 4 h. Cells were harvested by centrifugation and lysed by sonication. The proteins were further purified using a HiTrap chelating affinity column[15] previously loaded with metal ions (1 mL of 100 mM $NiCl_2$) and equilibrated with 50 mM Tris–HCl buffer (pH 7.2) and 10% glycerol. The column was washed with this buffer until the absorbance value at 280 nm was that of the buffer; then, the bound protein was eluted with 50 mM Tris–HCl buffer, pH 7.2, containing 500 mM imidazole and 10% glycerol. The fractions were dialyzed against 50 mM Tris–HCl buffer, pH 7.2. The amount of LigD, L, E, F, and G enzymes was estimated by absorbance at 280 nm using the determined molar extinction coefficients of 43.657, 34.167, 107.443, 89.117, and 90.436 M^{-1} cm^{-1}, respectively. Gel permeation chromatography was performed on a Superdex 200 column (GE Healthcare, Milano, Italy) using 50 mM potassium phosphate, pH 7.5, and 250 mM NaCl as elution buffer.

3.3 Activity and kinetic measurements

The specific activities of LigD and LigL were determined on racemic 1-(4-hydroxy-3-methoxyphenyl)-2-(2-methoxyphenoxy)-propane-1,3-diol (GGE) as substrate at 25 °C in 20 mM sodium acetate buffer, pH 9.0, in the presence of 0.5 mM NAD^+ following the absorbance change at 340 nm (*i.e.* as production of NADH). The apparent kinetic parameters were

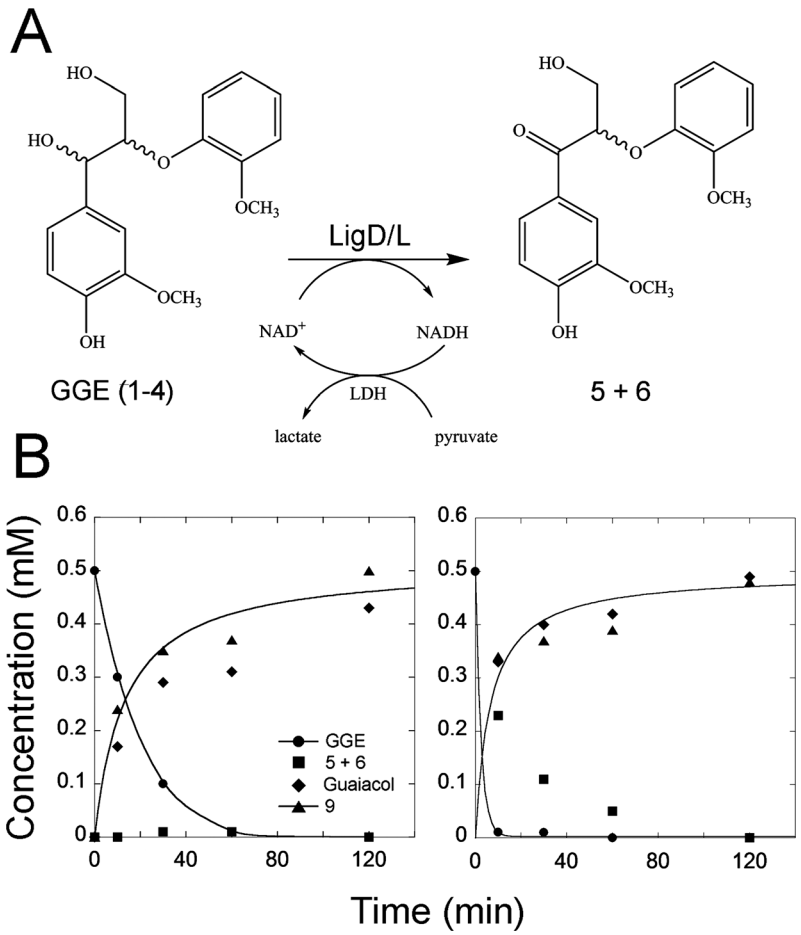

Fig. 7 A) Reaction mechanism scheme of NAD^+ recycling in the GGE oxidation step catalyzed by LigD, L. B) Time course of GGE oxidation catalyzed by LigD, L, E, F, G without (left) and with (right) recycling of NAD^+.

determined similarly using a fixed amount of enzyme and various substrate concentrations (0–5 mM): activity was analyzed with respect to substrate concentration according to the classical Michaelis–Menten equation or an equation modified to account for a substrate inhibition effect.[16,17]

The temperature dependence of LigD and LigL activity was investigated in the presence of 0.5 mM NAD^+ and 0.5 mM GGE at temperatures ranging from 15 to 60 °C. Enzyme stability was assessed at 25, 37, and 45 °C by incubating the enzyme solution in 20 mM sodium acetate buffer, pH 9.0. At different times, samples were withdrawn and residual activity was assayed.

The pH dependence of the activity towards GGE was determined by using the multicomponent buffer 15 mM Tris, 15 mM sodium carbonate, 15 mM phosphoric acid, and 250 mM potassium chloride adjusted to the appropriate pH with HCl or KOH in the pH range 4.0–9.0.[18] The dependence of enzyme stability was assessed by measuring the residual enzymatic activity after incubating the enzyme preparations at 25 °C for 24 hours at different pH values.

3.4 Spectral measurements

All fluorescence measurements were performed by using a 1 mL cell in a Jasco FP-750 instrument equipped with a thermostated cell holder (Jasco, Cremella, Italy). Tryptophan emission spectra were taken from 300 to 400 nm using an excitation wavelength of 280 nm; 5 and 10 nm bandwidths were used for excitation and emission, respectively. All spectra were corrected by subtracting the emission of the buffer. NAD^+ binding experiments were carried out at 15 °C and at 0.3 μM protein concentration: the change in emission at 340 nm was plotted as a function of ligand concentration.[19]

CD spectra were recorded on a J-810 Jasco spectropolarimeter and analyzed by means of Jasco software. The cell path was 1 cm for measurements in the 250 to 350 nm and 0.1 cm for measurements in the 190 to 250 nm region.[19] Proteins were in 50 mM Tris–HCl buffer, pH 7.5, containing 10% (v/v) glycerol. The secondary structure was estimated by using K2D3 software.[20]

Studies on the temperature sensitivity of tryptophan fluorescence (taken at 340 nm, as a reporter of tertiary structure modifications) were carried out using a software-driven, Peltier-based temperature controller, with a temperature gradient of 0.5 °C min^{-1}.[19,21] Temperature-induced loss of secondary structure was monitored by following the circular dichroism (CD) signal at 220 nm, recorded on a J-810 Jasco spectropolarimeter that was also equipped with a Peltier-

based temperature controller, which made it possible to reproduce the process at the same temperature gradient (0.5 °C min^{-1}) used in the fluorescence studies, and then analyzed by means of Jasco software.[19,21]

3.5 Determining extinction coefficients of purified Lig enzymes

The extinction coefficients of native proteins were determined using a Jasco FP-750 spectrophotometer. Here, appropriate dilutions of protein samples were completely denatured in 6 M urea,[19] assuming as extinction coefficients of the fully denatured proteins those calculated by ExPASy Bioinformatic Resource Portal (http://www.expasy.org/) using the ProtParam tool.

3.6 Chemical analyses

All chemicals and L-lactate dehydrogenase from rabbit muscle were purchased from Sigma-Aldrich (Milano, Italy). All solvents were of analytical grade.

HPLC analyses were performed on a Jasco apparatus with a Luna 5 μm C18(2) column (Phenomenex, Castel Maggiore, Italy), length/internal diameter = 150/4.6 mm, and UV detector set at 280 nm. A binary solvent system of solvent A, 17.5 mM sodium acetate buffer, pH 4.3/CH_3CN 95 : 5 (v/v), and solvent B, pure CH_3CN, was used with the following gradient (flow rate of 1 mL min^{-1}): 0–8 min, 90% A; 8–15 min, ramping up to 70% A; 15–25 min, 70% A; 25–35 min, ramping up to 90% A. The retention times (t_R) of 3-hydroxy-1-(4-hydroxy-3-methoxyphenyl)-propan-1-one (**9**), guaiacol, 1-(4-hydroxy-3-methoxyphenyl)-2-(2-methoxyphenoxy)propane-1,3-diol (GGE, **1**–**4**), and 3-hydroxy-1-(4-hydroxy-3-methoxyphenyl)-2-(2-methoxyphenoxy)propan-1-one (**5** + **6**) are 6.14 min, 14.5 min, 16.8 min, and 19.8 min, respectively. The calibration curves of GGE (**1**–**4**), guaiacol, (*R*,*S*)-3-hydroxy-1-(4-hydroxy-3-methoxyphenyl)-2-(2-methoxyphenoxy)-propan-1-one (**5** + **6**), and **9** are reported in Fig. S3 of the ESI.†

Chiral HPLC analyses shown in Fig. 4 were performed on an Agilent apparatus (Cernusco sul Naviglio, Italy) equipped with a UV detector set at 280 nm and fitted with a Chiracel OD 5 μm column (Phenomenex), length/internal diameter = 250/4.6 mm, eluent hexane/2-propanol 8 : 2, flow rate of 0.7 mL min^{-1}. Samples, 5 μL at 1 mg mL^{-1} concentration in THF, were injected into the column. The retention times (t_R) were as follows: guaiacol = 10.2 min; final product **9** = 14.4 min; **6** = 18 min; **5** = 22 min.

Chiral HPLC analyses shown in the insets of Fig. 5 (concerning compounds **5** and **6**) were performed on a Merck Hitachi apparatus L6200 equipped with a UV detector L4200 set at 280 nm and fitted with the Chiracel OD 5 μm column, eluent hexane/2-propanol 8 : 2, flow rate of 1.5 mL min^{-1}.

^1H NMR spectra were recorded on a Bruker AV 400 spectrometer (400 MHz) (Bruker, Milano, Italy) equipped with a 5 mm multinuclear probe and reverse detection spectrometer. ^1H NMR chemical shifts are reported in parts per million (ppm) in relation to Me_4Si. Mass spectra were recorded on an ESI/MS Bruker Esquire 3000 PLUS (Esi Ion Trap LC/MSn System), directly infusing a methanol solution of the compounds (infusion rate of 4 μL min^{-1}).

3.7. Synthesis of 1-(4-hydroxy-3-methoxyphenyl)-2-(2-methoxyphenoxy)-propane-1,3-diol (1–4) and 3-hydroxy-1-(4-hydroxy-3-methoxyphenyl)-propan-1-one (9)

GGE (**1**–**4**) was synthesized chemically according to a modified version of the one reported by Crestini and D'Auria[22] (see the ESI†). The results of the NMR and chiral HPLC analyses are reported in the ESI† and in Fig. S4.† The synthetic route of 3-hydroxy-1-(4-hydroxy-3-methoxyphenyl)propan-1-one (**9**) is reported in the ESI.†

3.8 Bioconversions

A 10 mM GGE substrate solution was prepared by dissolving 32 mg (0.1 mmol) of GGE in 10 mL of 20 mM ammonium acetate buffer (pH 9.0). The time course of bioconversions was determined by HPLC analysis: 100 μL of reaction mixture was stopped by adding 100 μL of a solution composed of 100 mM sodium acetate buffer (pH 4.3) and 50% CH_3CN, then centrifuged and separated; the supernatant was analyzed by HPLC.

- Bioconversion conducted at 45 °C (all the following concentrations are the final values):

1) GGE + LigD

a) 22 μL of enzyme LigD (0.1 mg mL^{-1}) were added to 50 μL of GGE solution (0.5 mM) and 50 μL of NAD^+ (0.5 mM) in 878 μL of 20 mM ammonium acetate buffer, pH 9.0.

b) 66 μL of enzyme LigD (0.1 mg mL^{-1}) were added to 150 μL of GGE solution (0.5 mM) and 15 μL of NAD^+ (0.5 mM) in 2.769 mL of 20 mM potassium phosphate buffer, pH 7.5.

- Bioconversions conducted at 25 °C:

2) GGE + LigL

75 μL of enzyme LigL (0.1 mg mL^{-1}) were added to 150 μL of GGE solution (0.5 mM) and 15 μL of NAD^+ (0.5 mM) in 2.760 mL of 20 mM ammonium acetate buffer, pH 9.0.

3) GGE + LigD + LigF

110 μL of enzyme LigD (0.1 mg mL^{-1}) were added to 250 μL of GGE solution (0.5 mM) and 250 μL of NAD^+ (0.5 mM) in 4.390 mL of 20 mM ammonium acetate buffer, pH 9.0. After 24 h 40 μL of LigF (0.1 mg mL^{-1}) and 200 μL of glutathione (0.5 mM) were added to the remaining reaction mixture (4.2 mL).

4) GGE + LigD + LigF + LigG

50 μL of enzyme LigD (0.1 mg mL^{-1}) were added to 50 μL of GGE (0.5 mM) and 50 μL of NAD^+ (0.5 mM) in 2.850 mL of 20 mM ammonium acetate buffer, pH 9.0. After 24 h 20 μL of LigF (0.1 mg mL^{-1}) and 10 μL of glutathione (0.5 mM) were added to the remaining reaction mixture (2.1 mL). After another 24 h, 40 μL of LigG solution (0.1 mg mL^{-1}) were added.

5) GGE + LigF + NAD^+

30 μL of enzyme LigF (0.1 mg mL^{-1}) were added to 150 μL of GGE (0.5 mM) and 150 μL of NAD^+ (0.5 mM) in 2.670 mL of 20 mM ammonium acetate buffer, pH 9.0.

6) GGE + LigD, L, F, E + LigG

20 μL of enzyme LigD (0.1 mg mL^{-1}), 18 μL of LigF (0.1 mg mL^{-1}), 75 μL of LigL (0.1 mg mL^{-1}), and 30 μL of LigE (0.1 mg mL^{-1}) were added to 150 μL of GGE (0.5 mM), 30 μL of NAD^+ (1 mM), and 30 μL of glutathione (1 mM) in 2.647 mL of 20 mM ammonium acetate buffer, pH 9.0. After 18 h 73.4 μL of LigG (0.2 mg mL^{-1}) and 29 μL of glutathione (1 mM) were added to the remaining reaction mixture (2.9 mL).

7) GGE + LigD, L, F, E, G

20 μL of enzyme LigD (0.1 mg mL^{-1}), 18 μL of LigF (0.1 mg mL^{-1}), 75 μL of LigL (0.1 mg mL^{-1}), 30 μL of LigE (0.1 mg mL^{-1}), and 76 μL of LigG (0.2 mg mL^{-1}) were added to 150 μL of GGE (0.5 mM), 30 μL of NAD^+ (1 mM) and 60 μL of glutathione (2 mM) in 2.541 mL of 20 mM ammonium acetate buffer, pH 9.0.

8) GGE + LigD, L, F, E, G, with recycling of NAD^+

20 μL of enzyme LigD (0.1 mg mL^{-1}), 18 μL of LigF (0.1 mg mL^{-1}), 75 μL of LigL (0.1 mg mL^{-1}), 30 μL of LigE (0.1 mg mL^{-1}), 76 μL of LigG (0.2 mg mL^{-1}), and 41.6 μL of L-lactate dehydrogenase (0.5 U) were added to 150 μL of GGE (0.5 mM), 15 μL of NAD^+ (0.5 mM), 60 μL of glutathione (2 mM), and 60 μL of pyruvate (1 mM) in 2.454 mL of 20 mM ammonium acetate buffer, pH 9.0.

4. Conclusions

The five Lig enzymes from *S. paucimobilis* SYK-6 involved in the cleavage of β-O-4 linkage have been successfully overexpressed in recombinant form in *E. coli* and purified by a single chromatographic step (20–80 mg of pure protein per liter of fermentation broth). The recombinant proteins were purified in a folded conformation, as demonstrated by the fluorescence and CD signals corresponding to the presence of secondary and tertiary structure elements (Fig. 3).

The NAD^+-dependent dehydrogenases LigD and LigL possess a similar, apparent maximal activity (at pH 9.0, 25 °C, and at fixed 0.5 mM NAD^+ concentration) and a substrate inhibition effect at a >0.5 mM GGE concentration (Fig. 1). Such an effect was not observed at 45 °C; however, this higher temperature is not suitable for bioconversion trials since the stability of LigL at temperature values >25 °C is low. This instability largely arises from the low stability of the secondary structure elements, whose alteration precedes by 3 °C the alteration in the tertiary structure (41.2 and 44.2 °C, see Table 2). All the other Lig enzymes were comparatively more thermostable than LigL, showing T_m values ≥48 °C: however, the instability of LigL defines the temperature for bioconversion experiments. Both LigD and LigL show higher activity at pH 9.0 (Fig. 2): this, and the observed stability of GGE, set the optimal value for the first step of bioconversion at pH 9.0.

Owing to the absence of a quick and simple activity assay for glutathione transferases LigE and LigF and for glutathione lyase LigG, the optimization of GGE bioconversion was investigated by HPLC analysis. The full conversion of 0.5 mM GGE was obtained in 2 hours in the presence of all five Lig enzymes, at pH 9.0 and 25 °C, indicating that LigG catalyzes the glutathione-dependent cleavage of both β(*R*)- and β(*S*)-thioether. This conclusion can be demonstrated by following the reaction of LigG on compounds **7** and **8**. It was previously reported that LigG is a stereospecific β-(*S*)-thioetherase since it had little or no activity as a β-thioetherase with the LigE/LigP-produced β(*S*)-*S*-glutathionyl-α-veratrylglycerone (GS-β(*S*)VG).[10] This latter work did not clarify the fate of such GSH-conjugated β-etherase pathway intermediates, and the presence of a racemase-like enzyme for the conversion of the inactive β-epimer to the GSH conjugate that is cleaved by LigG, or the presence of a second β-*S*-thioetherase with the reverse stereospecificity for GSH-dependent cleavage of the β(*S*)-isomer, was hypothesized. In recent work, LigG was used on a synthetic mixture of GS-β(*S*)VG and GS-β(*R*)VG (and not directly on the reaction products of LigD, E, L, and F enzymes), showing a stereopreference for the GS-β(*S*)VG diastereoisomer since a 5:1 molar excess of GS-β(*S*)VG:GS-β(*R*)VG was detected following LigG (0.26 mg mL^{-1}) thioether cleavage at pH 7.5 for 1 h in the presence of 0.1 mM tris(2-carboxyethyl)phosphine and 5% acetone.[10] This observation does not exclude that under steady-state and optimized conditions (pH 9.0 and 25 °C) LigG can act on both isomers to yield a full conversion of **7** and **8** and bypass the requirement of a racemase-like enzyme at the cellular level. Indeed, the recently solved 3D structure of LigG does not clarify the inferred stereoselectivity since such a conclusion arose from a docking analysis of the (*R*) and (*S*) configuration of the glutathione adduct that identified multiple positions for the ligand in the active site region, and not from the resolution of an experimental structure.[11]

Finally, the bioconversion process was optimized by including pyruvate and L-lactate dehydrogenase to recycle NADH produced by LigD and LigL, thus pushing the equilibrium of the first step of GGE oxidation. Our work follows the study of Reiter *et al.*[12] carried out with LigD, F, and G and the cofactor regeneration by NAD^+-dependent glutathione reductases. However, we aimed to convert all the enantiomers of GGE through the additional use of LigE and LigL. Our approach significantly increased the conversion of GGE from ≤50% in Reiter *et al.*[12] to ≈100% conversion under our experimental conditions and, because of the low amount of enzymes used (which are produced in large quantities as recombinant proteins in *E. coli*), represents an inexpensive enzyme cascade.

Previous studies reported a significant increase in monomer release for softwood alkali-lignin after treatment with LigD, F, and G, although they were not active on bagasse organosolv lignin, probably because of the low β-aryl ether content or the enzyme inhibition effects.[12] Although the use of β-etherases for lignin processing is still in its infancy, the possibility of employing the full multienzymatic Lig system in combination with known ligninolytic enzymes on various lignin samples is currently under evaluation since the cleavage of the β-O-4 aryl ether linkages is of utmost importance: these bonds constitute about 50% of all ethers in various lignins and their breakdown could result in the production of

smaller phenolic compounds that could be used in preparative organic chemistry (here, it should be mentioned that LigD is active on a wide range of β-O-4 linked dimers and oligomers, including genuine dilignols).[14] The combination of these enzymes would provide a great opportunity to transform lignin, which is the cheapest and most abundant aromatic material in nature, into promising feedstocks of aromatic compounds as an alternative to the oil source.

Acknowledgements

This work was performed as part of the ValorPlus project (P. D. and L. P.) that has received funding from the European Union's Seventh Framework Programme for research, technological development and demonstration under grant agreement no. FP7-KBBE-2013-7-613802, and Biorefill project (Regione Lombardia) (L. P.). C. A. is a PhD student of the Research Doctorate Program in Chemical Engineering and Industrial Chemistry at Politecnico di Milano.

References

1 M. P. Pandey and C. S. Kim, *Chem. Eng. Technol.*, 2011, **34**, 29–41.
2 T. Kleine, J. Buendia and C. Bolm, *Green Chem.*, 2013, **15**, 160–166.
3 T. vom Stein, T. Weigand, C. Merkens, J. Klankermayer and W. Leitner, *ChemCatChem*, 2013, **5**, 439–441.
4 C. Sanchez, *Biotechnol. Adv.*, 2009, **27**, 185–194.
5 L. Pollegioni, F. Tonin and E. Rosini, *FEBS J.*, 2015, **282**, 1190–1213.
6 Y. Otsuka, T. Sonoki, S. Ikeda, S. Kajita, M. Nakamura and Y. Katayama, *Eur. J. Biochem.*, 2003, **270**, 2353–2362.
7 P. Picart, C. Müller, J. Mottweiler, L. Wiermans, C. Bolm, P. Domínguez de María and A. Schallmey, *ChemSusChem*, 2014, **7**, 3164–3171.
8 E. Masai, Y. Katayama, S. Nishikawa, M. Yamasaki, N. Morohoshi and T. Haraguchi, *FEBS Lett.*, 1989, **249**, 348–352.
9 Y. Sato, H. Moriuchi, S. Hishiyama, Y. Otsuka, K. Oshima, D. Kasai, M. Nakamura, S. Ohara, Y. Katayama, M. Fukuda and E. Masai, *Appl. Environ. Microbiol.*, 2009, **75**, 5195–5201.
10 D. L. Gall, H. Kim, F. Lu, T. J. Donohue, D. R. Noguera and J. Ralph, *J. Biol. Chem.*, 2014, **289**, 8656–8667.
11 E. Meux, P. Prosper, E. Masai, G. Mulliert, S. Dumarçay, M. Morel, C. Didierjean, E. Gelhaye and F. Favier, *FEBS Lett.*, 2012, **586**, 3944–3950.
12 J. Reiter, H. Strittmatter, L. O. Wiemann, D. Schieder and V. Sieber, *Green Chem.*, 2013, **15**, 1373–1381.
13 E. Masai, A. Ichimura, Y. Sato, K. Miyauchi, Y. Katayama and M. Fukuda, *J. Bacteriol.*, 2003, **185**, 1768–1775.
14 Y. Tsuji, R. Vanholme, Y. Tobimatsu, Y. Ishikawa, C. E. Foster, N. Kamimura, S. Hishiyama, S. Hashimoto, A. Shino, H. Hara, K. Sato-Izawa, P. Oyarce, G. Goeminne, K. Morreel, J. Kikuchi, T. Takano, M. Fukuda, Y. Katayama, W. Boerjan, J. Ralph, E. Masai and S. Kajita, *Plant Biotechnol. J.*, 2015, **13**, 821–832.
15 F. Volontè, F. Marinelli, L. Gastaldo, S. Sacchi, M. S. Pilone, L. Pollegioni and G. Molla, *Protein Expression Purif.*, 2008, **61**, 131–137.
16 L. Pollegioni, S. Lorenzi, E. Rosini, G. L. Marcone, G. Molla, R. Verga, W. Cabri and M. S. Pilone, *Protein Sci.*, 2005, **14**, 3064–3076.
17 E. Rosini, C. S. Monelli, L. Pollegioni, S. Riva and D. Monti, *J. Mol. Catal. B: Enzym.*, 2012, **76**, 52–58.
18 C. M. Harris, L. Pollegioni and S. Ghisla, *Eur. J. Biochem.*, 2001, **268**, 5504–5520.
19 L. Caldinelli, S. Iametti, A. Barbiroli, F. Bonomi, D. Fessas, G. Molla, M. S. Pilone and L. Pollegioni, *J. Biol. Chem.*, 2005, **280**, 22572–22581.
20 C. Louis-Jeune, M. A. Andrade-Navarro and C. Perez-Iratxeta, *Proteins*, 2012, **80**, 374–381.
21 L. Pollegioni, S. Iametti, D. Fessas, L. Caldinelli, L. Piubelli, A. Barbiroli, M. S. Pilone and F. Bonomi, *Protein Sci.*, 2003, **12**, 1018–1029.
22 C. Crestini and M. D'Auria, *Tetrahedron*, 1997, **53**, 7877–7888.